

Automated Detection of Singularity from Orientation Map of Isoclinics in Digital Photoelasticity

Pichet Pinit

Department of Mechanical Technology Education
Faculty of Industrial Technology Education and Technology
King Mongkut's University of Technology Thonburi
Bangmod, Toongkru, Bangkok 10140, Thailand
Tel: 0-2470-8526, E-mail: ipichet@yahoo.com

Abstract

In digital photoelasticity, the determination of the isoclinic parameter in its physical range is still the difficult problem. A recent work proposed by the author and his co-worker can effectively unwrap the orientation map regardless the existence of the singularity. The technique involves the detection of the singularity and the preservation of them for final processing with a certain limitation. In this paper, a method for accurately detecting the positions of the singularity is proposed and evaluated with the orientation maps of the circular ring under compressive load obtained on the basis of the phase-shifting technique. Experimental results are also presented and discussed.

Keywords: Digital photoelasticity, Directional Map, Orientation Map, Phase-shifting technique, Singularity

1. Introduction

Photoelasticity is a powerful experimental technique which enables a complete stress analysis to be carried out on engineering structural components at the design stage. However, the analysis can be tedious process and is normally only carried out by an expert. At present day, the field of digital photoelasticity has been developed by integrating a new data acquisition and data processing to the conventional photoelasticity.

In digital photoelasticity, two fringe patterns, i.e., an isoclinic fringe pattern and an isochromatic fringe pattern, are given in the form of a digital image (an intensity data). These fringe patterns provide both magnitude and directions of stresses. The isoclinic fringe pattern enables the isoclinic parameter ϕ , which directly relates to the principal stress directions or directional map, to be determined whereas the isochromatic fringe pattern enables the isochromatic parameter δ , which directly relates to $(\sigma_1 - \sigma_2)$, to be evaluated.

For ϕ , a number of automated whole-field approaches have been proposed to determine it, particularly the whole-field method based on phase-shifting technique (PST) [1]. By PST, two problems arise when calculating ϕ , i.e., the isochromatic-isoclinic interaction [1] and wrapped phase map. The first problem occurs because of

the unreliability of the isoclinic parameter at and near the isochromatic fringe skeleton. The wrapped phase data arises because only unambiguous phase is known at most in the range $(-\pi/4, +\pi/4]^*$ instead of $(-\pi/2, +\pi/2]$.

For the wrapped isoclinics, if it is left unsolved, the ambiguity exists on whether the map of isoclinics shows σ_1 or σ_2 directions over the entire domain. That this map of wrapped isoclinics can refer to both principal-stress directions leads to the name 'orientation map'.

To bring ϕ to its physical range, a phase unwrapping (PU) is necessary. Recently, PU was proposed to unwrap the map of wrapped in which the singularity was taken in the consideration [2]. In that work, the crucial step is to detect the singularity and only one orientation map was used. The binary mask image representing the points detected shows some erroneous detected positions.

In this paper, the detection of such points based on the combination of the orientation maps is present. The detection technique is applied to the problem of circular ring under compression.

2. Computation of Principal-stress Directional Field

2.1 Theoretical aspect

The theoretical expression of the isoclinic parameter ϕ is well known as

$$\tan 2\phi = \frac{2\tau_{xy}}{\sigma_{xx} - \sigma_{yy}} \quad (1)$$

where σ_{xx} , σ_{yy} and τ_{xy} are the two-dimensional stress components in the Cartesian coordinates.

Then, for ϕ , inverting Equation (1) yields

$$\phi = \frac{1}{2} \arctan \left(\frac{2\tau_{xy}}{\sigma_{xx} - \sigma_{yy}} \right) \quad (2)$$

Equation (2) provides $\phi \in (-\pi/4, +\pi/4]$ by using the ordinary arctangent operation. It should be noted here that even though Equation (1) is theoretically derived, the ambiguity always exists unless PU is applied.

* $(a, b]$ represents $a < x \leq b$ in which x is a variable of interest.

the Cartesian stress components in Equation (2) [1]

Stress condition	Singularity	
$\sigma_{xx} = \sigma_{yy} \neq 0$ and $\tau_{xy} = 0$	isotropic point	1
$\sigma_{xx} = \sigma_{yy} = 0$ and $\tau_{xy} = 0$	singular point	
$\sigma_{xx} = \sigma_{yy} = \infty$ and $\tau_{xy} = \infty$	pole	

2.2 Experimental aspect based on photoelasticity

An equation of the intensity I for different angular positions θ at the steps m of the dark-field plane polariscope with the white light source (Figure 1) can be expressed as [1]

$$I_{m,\lambda} = I_{\text{mod},\lambda} \sin^2 2(\phi - \theta) + I_{\text{b},\lambda} \quad (3)$$

where

$$I_{\text{mod},\lambda} = \frac{1}{\Delta\lambda} \int_{\lambda_1}^{\lambda_2} I_{\text{p},\lambda} \sin^2(\pi N_\lambda) d\lambda \quad (4)$$

λ (= R, G, B) is the primary wavelengths of the white light source, $\Delta\lambda = \lambda_2 - \lambda_1$ in which λ_2 and λ_1 are the upper and lower limits of the spectrum of the light, $I_{\text{p},\lambda}$ is the light coming out of the polarizer, N_λ ($= \delta_\lambda / 2\pi$) is the relative fringe order and $I_{\text{b},\lambda}$ is the background intensity.

The expression for the orientation field of isoclinics based on the application of the four-step phase shift method to Equation (3) for $m = 1, 2, 3$, and 4 can be written as [2, 3]

$$\phi_w = \frac{\pi}{8} - \frac{1}{4} \arctan \left(\frac{I_1^s - I_3^s}{I_2^s - I_4^s} \right) \quad \text{for } I_{\text{mod}}^s \neq 0 \quad (5)$$

where

$$I_m^s = \sum_{\lambda} I_{m,\lambda} = I_{m,\text{R}} + I_{m,\text{G}} + I_{m,\text{B}} \quad (6)$$

$$I_{\text{mod}}^s = I_{\text{mod},\text{R}} + I_{\text{mod},\text{G}} + I_{\text{mod},\text{B}} \\ = \sqrt{(I_1^s - I_3^s)^2 + (I_2^s - I_4^s)^2} \quad (7)$$

The subscript 'w' denotes that ϕ is of wrapped isoclinics of the range $(0, +\pi/4]$ due to the use of the ordinary arctangent operation.

3. Definition of Singularity

The singularity is one of the properties of the orientation or the directional field of isoclinics in which the state of stresses satisfies certain conditions. The following well-known theoretical formula will help in an explanation of the formation of the singularity.

$$\sigma_1, \sigma_2 = \frac{\sigma_{xx} + \sigma_{yy}}{2} \pm \frac{1}{2} \sqrt{(\sigma_{xx} - \sigma_{yy})^2 + 4\tau_{xy}^2} \quad (8)$$

As seen in Equation (2), there are three cases that can cause the singularity in such orientation or directional field of the isoclinics.

3.1 Isotropic point

A point at which the state of stresses satisfies the first condition shown in Table 1 is called an isotropic point [4]. At this point, $\sigma_1 = \sigma_2 = \sigma \neq 0$ (Equation (8)) and, consequently, ϕ is indeterminate at such point (Equation

(2)). However, this indetermination means that the isoclinics of all different parameters of ϕ can pass through and intersect each other at the point.

This can be explained by considering the following expression of the shear stress τ in terms of the principal stress difference.

$$\tau = \left(\frac{\sigma_1 - \sigma_2}{2} \right) \sin(2\phi) \quad (9)$$

Since at the principal plane at which the principal stresses act, no shear stresses act on the plane; therefore, $\tau = 0$. Considering Equation (9) reveals that $\tau = 0$ regardless of the values of ϕ when $(\sigma_1 - \sigma_2) = 0$. It should be noted further that to satisfy the condition $\sigma_1 = \sigma_2 = \sigma \neq 0$ and $(\sigma_1 - \sigma_2) = 0$, the magnitude and the sign of the principal stresses must be the same. As a result, at the isotropic point, the state of the stress is of hydrostatic.

Since the physical range of isoclinics is of $(-\pi/2, +\pi/2]$ with modulo $+\pi$, then, in the map of the directional field, the line representing the end of this period as an abrupt isoclinic jump appears only one side of the isotropic point if such point is of a first order [1].

For other maps of orientation field (e.g., $[0, +\pi/2]$, $(-\pi/4, +\pi/4]$, and so on), there are at least two lines of abrupt isoclinic jumps passing through the isotropic point. These abrupt isoclinic jumps have the same signs. These signs identify the type of the isotropic point, i.e., positive or negative type.

If the isotropic point is of positive type, the isoclinics gradually vary around such point counterclockwise. In contrast, that point is of negative type if the isoclinics change the values clockwise around it [5].

3.2 Singular point

If the state of stresses of a point satisfies the second condition shown in Table 1, such point is called a singular point. The singular point may be considered to be a special case of the isotropic point since it is a point at which $\sigma_1 = \sigma_2 = 0$.

The singular point always lies on a shear-free boundary (Equation (9)). Therefore, the isoclinics of some parameters ϕ converge at the singular point. The reason is that at such boundary one of the principal stresses being normal to the boundary does not exist. Therefore, to satisfy the condition $\sigma_1 = \sigma_2 = 0$, the singular point must lie on such shear-free boundary.

The appearance of the lines representing the abrupt isoclinic jumps converging at the singular point is similar to those of the isotropic point. However, it may be difficult to exactly determine the singular point because the position on the model boundary at which the isoclinics converge strongly depends not only on the load condition but also on the geometrical shape of the model studied.

Under some circumstances, the singular point expresses itself as a series of points or a singular line. The circular disk under diametral compression possesses the

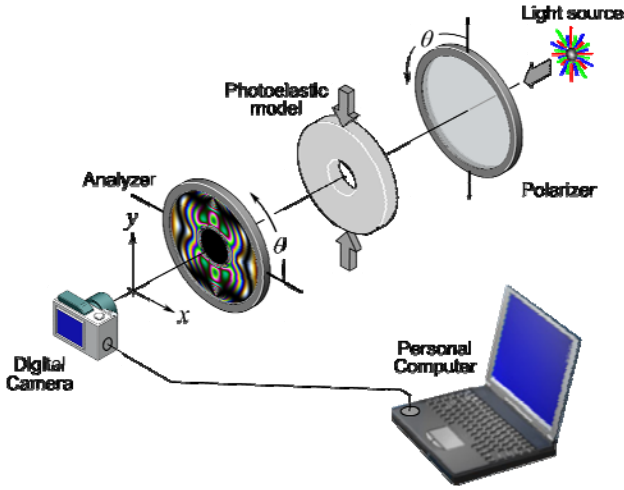


Figure 1. Dark-field plane polariscope system with the white light source having the circular ring model being placed inside and vertically loaded by a force.

singular line along its boundary. However, it is not an issue here because of the lack of the presence of the isotropic point.

The singular point usually shows a change of the signs of stresses, i.e., a transition from tension to compression and vice versa. Furthermore, the singular point is always of negative type [1].

3.3 Load application point and support (poles)

A point at which the applied load acts is known as an action point whereas a point at the support is termed as a reaction point. However, they are known as poles [4]. The state of stresses at these points is of the last condition shown in Table 1. At them, the principal-stress difference $(\sigma_1 - \sigma_2)$ approaches $+\infty$.

Since, by nature, the poles behave as though they were the singular point, then, the number of the lines representing the abrupt isoclinic jumps converging at the poles is also difficult to predict; however, unlike the singular point, the poles are of positive type [2].

4. Modulated Intensity

As seen in Equation (4), $I_{\text{mod},\lambda}$ is the function of the wavelength λ and the fringe order N_λ by which the relation between the fringe order and the principal-stress difference is expressed as [1]

$$N_\lambda = \frac{\delta_\lambda}{2\pi} = \frac{h}{f_{\sigma,\lambda}}(\sigma_1 - \sigma_2) \quad (10)$$

where h is the thickness of the model studied and $f_{\sigma,\lambda}$ is the well-known material stress fringe value obtained by calibration at wavelength λ .

Since, at the isotropic point and the singular point, $(\sigma_1 - \sigma_2) = 0$, then, at such points $N_\lambda = I_{\text{mod},\lambda} = I_{\text{mod}}^s = 0$ (see Equations. (4) and (10)). This is the condition of the zeroth-order fringe. Then, the isotropic point and the singular point are seen as dark spots or regions in the map of the modulated intensity regardless of the wavelengths used. By this fact, I_{mod}^s can be used to detect such points.

It is worthy to note that when dealing with the real

Table 2. Values of parameters used in the detection of the singularity [2]

Parameter	Value
T_{mod}	0.1
Detecting mask window, $w_{m \times n}^d$	$w_{21 \times 21}^d$

data, the condition may not give the correct positions because, at such points, the intensity may not be exact zero. As a result, it is possible to apply a tolerance to cope with this situation.

Then, if the values of I_{mod}^s at any point or pixel in the map is less than that of $T_{\text{mod}} I_{\text{mod},\text{max}}^s$, where T_{mod} is a predefined threshold or tolerance having values between 0.1 to 0.2 and $I_{\text{mod},\text{max}}^s$ is the maximum value of the map of I_{mod}^s , such pixel is considered to be the singularity, especially the isotropic and singular points.

5. Method of Detection of Singularity

The method of detection of the singularity is as followings.

- Detection of the singularity-to-be pixels: this is done by performing a raster scan over the orientation maps of the ranges $[0, +\pi/2]$ and $(-\pi/4, +\pi/4]$ using a mask window $w_{m \times n}^d$ and over the map of modulated intensity with the condition $T_{\text{mod}} I_{\text{mod},\text{max}}^s$. The pixels detected are separately stored into three binary arrays, i.e., $A_{[0, +\pi/2]}$, $A_{(-\pi/4, +\pi/4]}$ and A_{mod} , respectively. Note that these arrays are initially populated with one value and for the singularity the corresponding pixels are reset to zero value.
- Selection of the singularity: since, in all those three arrays, the pixels representing the positions of the singularity have the zero value, then, for clarity, let the parameters α , β and γ , respectively, be the pixel values in those three arrays. Also let A_{sin} be another binary array for storing final results which is initially populated with one value. Two following operations are of interest and they are:

(1) Doublet function $D(\alpha, \beta)$. For the same position of two pixels in both arrays $A_{[0, +\pi/2]}$ and $A_{(-\pi/4, +\pi/4]}$, if $D(\alpha, \beta) = D(0, 0)$, the pixel in array A_{sin} is assigned to be the singularity by setting it to zero value.

(2) Triplet function $T(\alpha, \beta, \gamma)$. For the same position of three pixels in the arrays $A_{[0, +\pi/2]}$, $A_{(-\pi/4, +\pi/4]}$, and A_{mod} , if $T(\alpha, \beta, \gamma) = T(0, 0, 0)$, the pixel in array A_{sin} is assigned to be the singularity by setting it to zero value.

6. Results and Discussion

The dark-field plane polariscope system used is the same as that already reported [2] and it is graphically shown in Figure 1. To examine the proposed method, it was applied to the problem of the circular ring under

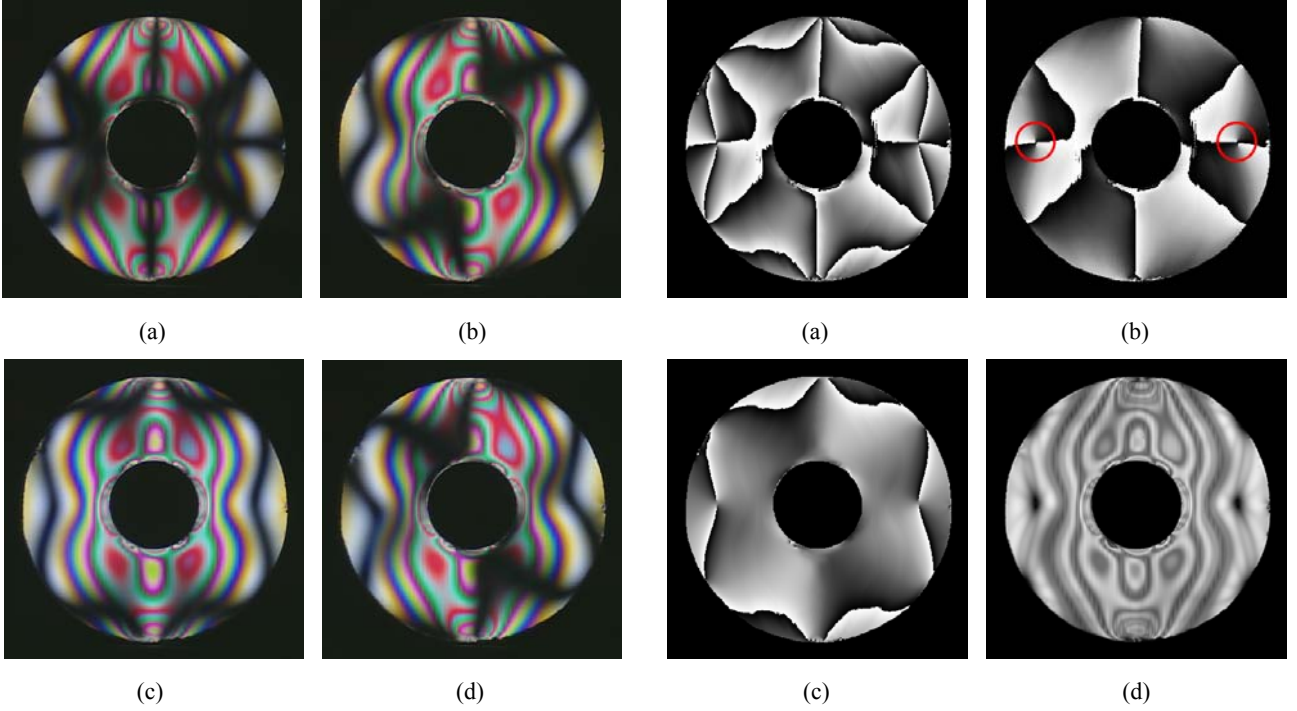


Figure 2. Experimentally generated color photoelastic fringe images of circular ring for four different angular configurations of the crossed polarizer and analyzer. (a) $\theta = 0$, (b) $\theta = +\pi/8$, (c) $\theta = +\pi/4$, and (d) $\theta = +3\pi/8$. (Printed in black and white.)

diametral compression. The model was made of 6-mm thick epoxy resin plate with 10-mm inner and 30-mm outer diameters.

Once the model was properly placed in the polariscope system and loaded by a force P of 274 N, the four photoelastic fringe images were digitally collected for four different configurations of the polariscope. Figure 2 shows these fringe images. The digital camera used for the collection of the color photoelastic fringe images was of Nikon model D70.

Figure 3(a) shows the resultant map obtained after applying Equation (5) to Figure 2 with normalization [2, 3]. It should be noted that this orientation map shows $\phi_w \in [0, +\pi/4]$. Figures 3(b)-(c) report the orientation maps of the range $[0, +\pi/2]$ and $(-\pi/4, +\pi/4]$, respectively. They were obtained from Figure 3(a) using the simple logic operations [2]. Figure 3(d) displays the map of I_{mod}^s . It should be noted here that this model contains two isotropic points and eight singular points [5].

Close scrutiny of Figures 3(a)-(c) reveals that the lines representing the abrupt isoclinic jumps are not smooth as they should be. This is because the isochromatic-isoclinic interaction. That is, Equation (5) is theoretically invalid when $I_{\text{mod}}^s = 0$; however, for the experimental data, the true condition is $I_{\text{mod}}^s \approx 0$. Hence, the closer are the values of I_{mod}^s to zero; the more obvious is the effect of the isochromatics on the maps of the isoclinics.

Comparing Figures 3(a)-(d) to (e) shows that the positions of the isotropic points, singular points and poles are clearly observed, particularly, the isotropic points (see

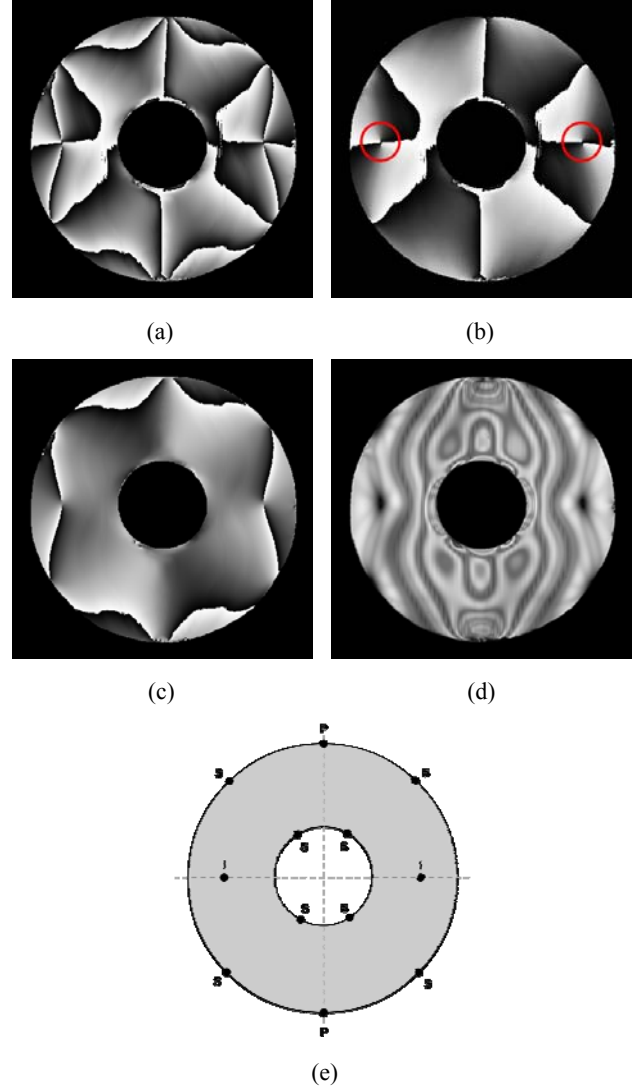


Figure 3. Orientation maps and Modulated intensity map. (a) orientation map $[0, +\pi/4]$, (b) orientation map $[0, +\pi/2]$, (c) orientation map $(-\pi/4, +\pi/4]$, (d) modulation map and (e) position of the singularity. 'I', 'S' and 'P' label the isotropic points, singular points and poles, respectively. The values of the modulated intensity and of isoclinics are separately and linearly converted into the 256-gray levels where 0 represents deep black and 255 represents pure white.

circles in Figure 3(b)). However, the four singular points lying on the inner boundary are rather vague. The other four singular points lying on the outer boundary are seen since the lines representing the abrupt isoclinic jumps pass through them (Figures 3(a)-(c)). Their positions can be also observed in Figure 3(d) as the dark regions making the outer boundary incomplete.

Figure 4 shows the binary images representing the positions of the singularity. Figure 4(a) was the result of the raster scan over Figure 3(b) whereas Figure 4(b) was obtained by performing the raster scan over Figure 3(c). Figure 4(c) shows the map of the singularity found by the condition $T_{\text{mod}} I_{\text{mod,max}}^s$. These maps were obtained using the parameters shown in Table 2. Figures 4(d) and (e)

report the results obtained by $D(\alpha, \beta)$ and $T(\alpha, \beta, \gamma)$, respectively.

Observing Figures 4(a) and (b) reveal that the isotropic points and poles were correctly detected. This can be confirmed by considering Figure 4(c). However, there are other detected positions that are not of the singularity (see circles in Figure 4(a)). As seen, these erroneous regions do not appear in Figure 4(b) since the isoclinics around the regions are continuous (Figure 3(c)).

After completely performing the doublet function, the erroneous regions were discarded whereas as for the triplet function, the map shows only the isotropic points and small dark region at the bottom (Figure 4(e)). It should be noted that at the poles, $(\sigma_1 - \sigma_2)$ approaches $+\infty$; thus, such small dark region appeared in Figure 4(e) is not the result of the condition $T_{\text{mod}} I_{\text{mod,max}}^s$. However, due to the applied load, the geometrical shape of the model at the poles may be slightly deformed and this effect makes a variation in the values of I_{mod}^s . As a result, some values of I_{mod}^s may be lower than such condition and then it was found as the singularity (considering Figure 4(c) for the bottom portion). It is informative noting that the poles can be only detected by using the abrupt isoclinic jumps around them (Figures 4(a) and (b)).

For the use of $T_{\text{mod}} I_{\text{mod,max}}^s$, the isotropic points were accurately detected as the two dark regions in Figure 4(c). Nevertheless, the position of the singular points are not clear but they can be seen if one makes a scrutiny on Figure 4(c) and compare to Figure 3(d) for the dark regions lying on the outer boundary. Figure 4(f) shows the unwrapped phase map in the physical range $(-\pi/2, +\pi/2]$. As seen, the directional field around the isotropic points is correct.

7. Conclusions

In this paper, the automated technique for detection of the singularity has been presented. The technique involves the use of the two orientation maps of the ranges $[0, +\pi/2]$ and $(-\pi/4, +\pi/4]$ and the map of modulated intensity I_{mod}^s . Results of the binary images show that isotropic points can be correctly found using the triplet function whereas the singular points and poles are detected by the doublet function.

Due to the mechanical stable at the isotropic points and the singular points, this would give a practical benefit for the optimum design of the structural members with holes for which they are made for wiring, reducing the weight of the structures and/or connecting them by fasteners (Figures 4(c) and (e)).

However, in the view of PU, the directional map obtained only using the doublet function is good for PU requirements [2]. That is, as seen in Figure 4(d), the isotropic points, singular points and pole are found. Since they can cause failure of PU, totally finding them makes PU more stable.

It is seen that Figure 4(b) can also be used in PU as in the case Figure 4(d) because they look alike. However, this similarity may not happen of other models; therefore, the use of the results obtained from the doublet function is more appropriate.

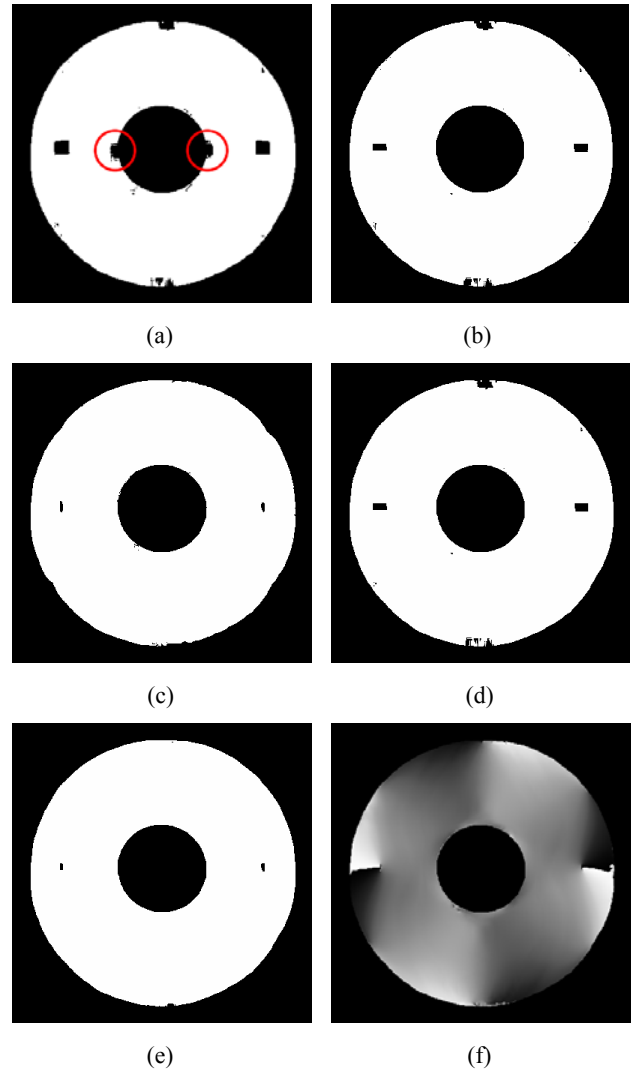


Figure 4. Binary images representing the singularity obtained from (a) $A_{[0, +\pi/2]}$, (b) $A_{(-\pi/4, +\pi/4]}$, (c) A_{mod} , (d) A_{sin} by $D(\alpha, \beta)$, (e) A_{sin} by $T(\alpha, \beta, \gamma)$ and (f) directional map of the range $(-\pi/2, +\pi/2]$ by which black represents $-\pi/2$ and white represents $+\pi/2$.

References

- [1] Ramesh, K., 2000. Digital Photoelasticity: Advanced Techniques and Applications. Springer, New York.
- [2] Pinit, P., and Umezaki, E., 2007. Digitally whole-field analysis of isoclinic parameter in photoelasticity by four-step color phase-shifting technique. Optics and Lasers in Engineering, Vol. 45, No. 7, pp. 795-807.
- [3] Pinit, P. and Umezaki, E., 2005. Full-field determination of principal-stress directions using photoelasticity with plane polarized RGB lights, Optical Review, Vol. 12, No. 3, pp. 228-232.
- [4] Umezaki, E., Waranabe, H., Sirichai, S. and Shimamoto, A., 1994. Extraction of singular points from photoelastic measurement, *Recent Advances in Experimental Mechanics* (Gomes, S., et al., eds.), Rotterdam, Netherlands, pp. 107-112.
- [5] Frocht, M.M., 1948. Photoelasticity, Vol. 1, John Wiley & Sons, New York.

